Supplement of Hydrol. Earth Syst. Sci., 29, 2997–3018, 2025
https://doi.org/10.5194/hess-29-2997-2025-supplement

Hydrology and Earth System Sciences
Open Access
EGU

Supplement of

Self-potential signals related to tree transpiration in a Mediterranean climate

Kaiyan Hu et al.

Correspondence to: Damien Jougnot (damien.jougnot@upmc.fr)

Description of the Supplementary Material

Figure S1 presents the Fourier spectrum analysis of sap velocity and SP data collected from January 1, 2023, to January 1, 2024 for Aleppo pine (FBPh) and Holm oak (FBQi) at the Font-Blanche site.

Figure S2 displays the correlation coefficients between tree data (SP and sap velocity) and meteorological data (precipitation, air temperature, actual evapotranspiration, global radiation and vapor pressure deficit) at the Font-Blanche site. The raw tree SP data were downsampled to a 30-min interval to calculate the Pearson correlation coefficient between it with other half-hourly measured data (see Table S1).

Figure S3 shows the one-year data collected at the Larzac and LSBB sites throughout 2023, including continuous measurements of sap velocity and SP in two oaks. There are missing sap velocity data for LaQp in July. Daily meteorological data collected at the LSBB site end on July 30, 2023.

Figure S4 presents wavelet coherence maps between sap velocity and SP data collected throughout 2023 on the Pubescent oak (LaQp) at the Larzac site and the Holm oak (LSQi) at the LSBB site.

Figure S5 presents the test results of using different total numbers of modes to decompose tree SP data on the Holm oak (FBQi) at the Font-Blanche site using the VMD method. The second-last decomposed modes of tree SP data under different totals show similar amplitudes and patterns in a diurnal rhythm.

Figure S6 exhibits the frequency spectra of six decomposed modes of tree SP and sap velocity data collected on the Aleppo pine (FBPh) at the Font-Blanche site using the VMD method.

Figure S7 includes the Pearson correlation coefficients between the decomposed sub-signals collected at the Font-Blanche site within April 16–30, 2023.

Figure S8 presents estimates of the effective excess charge density of xylem vessels over two-week periods in different seasons of 2023 for Aleppo pine (FBPh) and Holm oak (FBQi) at the Font-Blanche site.

Figure S9 suggests an experimental setup describing how SP electrodes equipped on the trunk may obtain duplicated measurements and analyse the electrode-related effects.

Figure S10 shows relationships between the fifth decomposed modes of sap velocity (VMD_5^{SV}) and tree SP (VMD_5^{SP}) signals in four seasons of 2023 for the Holm oak (FBQi) at the Font-Blanche site.

Figure S11 recommends a tree electrode configuration.

Table S1 includes different parameters of measurements and the corresponding sampling time interval.

Table S2 includes the detailed characteristics of relationships between sap velocity and SP in different seasons of 2023

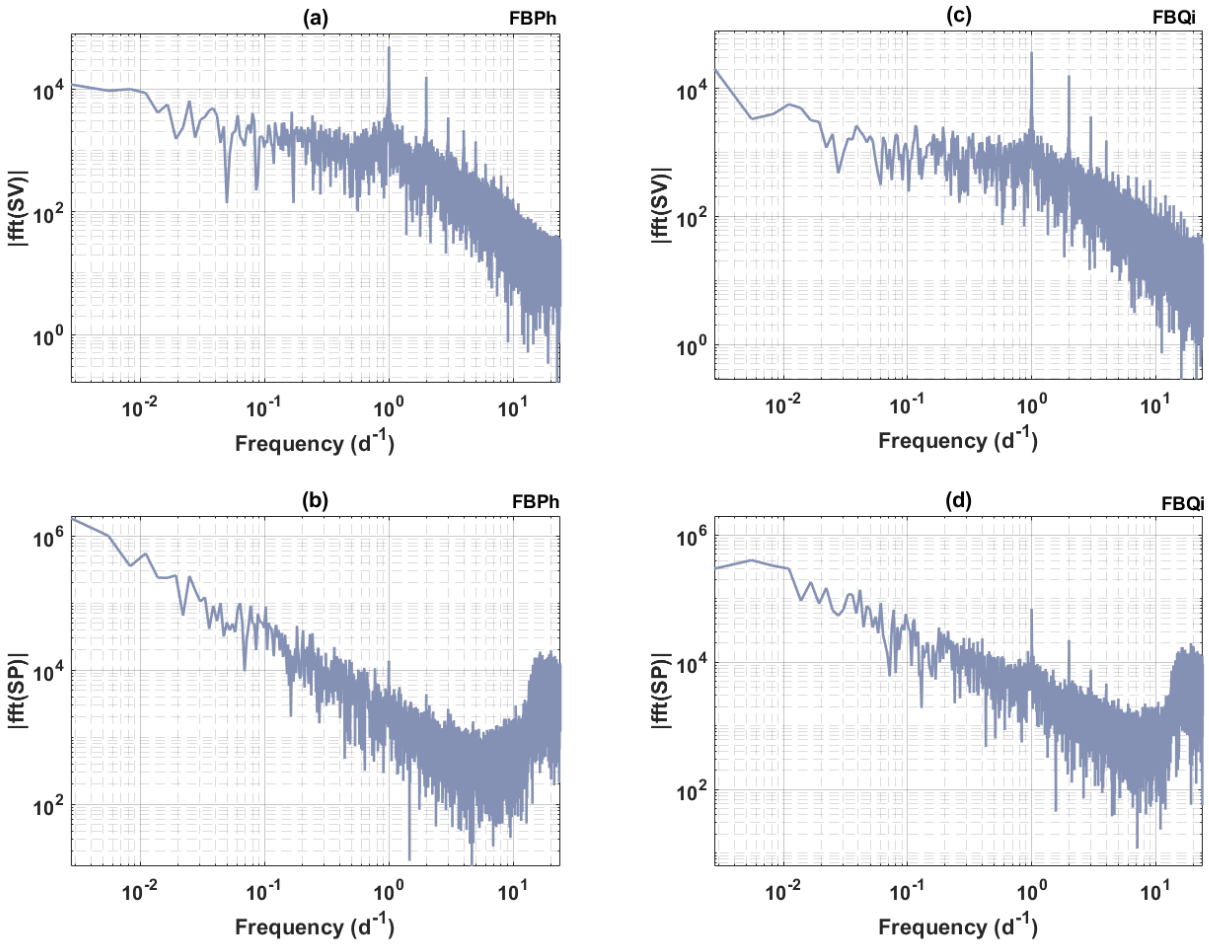

Figure S1: Magnitude of sap velocity (SV) and SP spectra obtained using a fast Fourier transform algorithm. (a, c) SV and SP spectra for Aleppo pine (FBPh). (b, d) SV and SP spectra for Holm oak (FBQi). Data were collected from January 1, 2023, to January 1, 2024 at the Font-Blanch site.

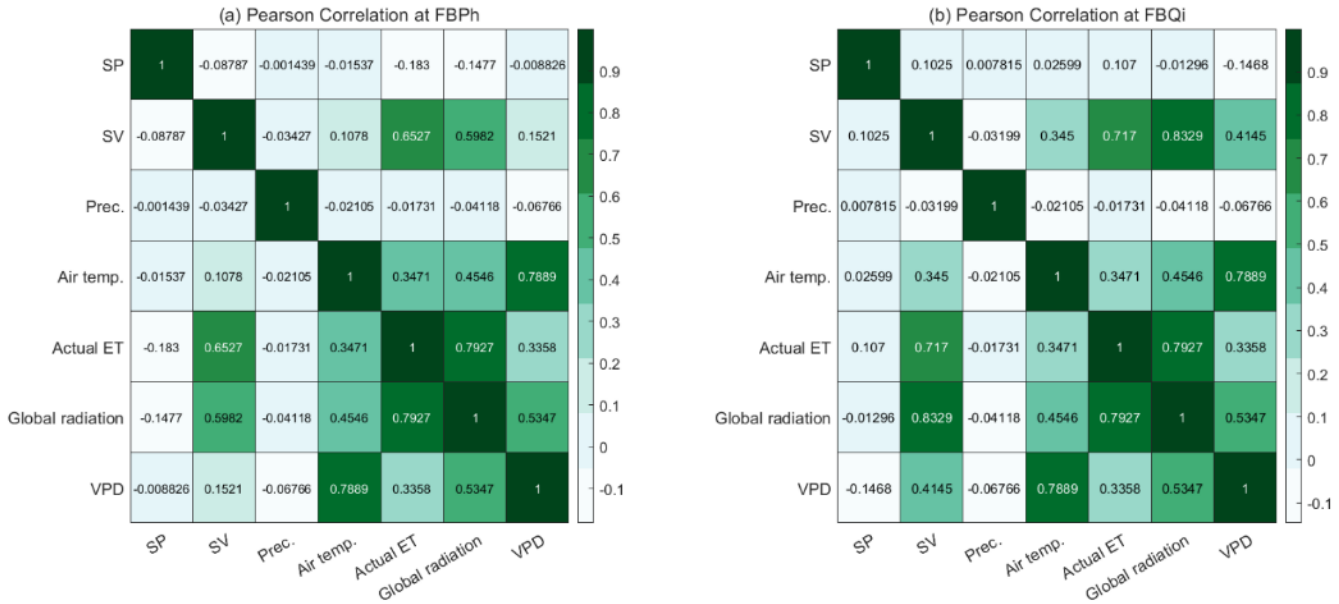

Figure S2: The correlation coefficients of the time-varying data at the Font-Blanche site. (a–b) Pearson correlations on Aleppo pine (a) and Holm oak (b), respectively

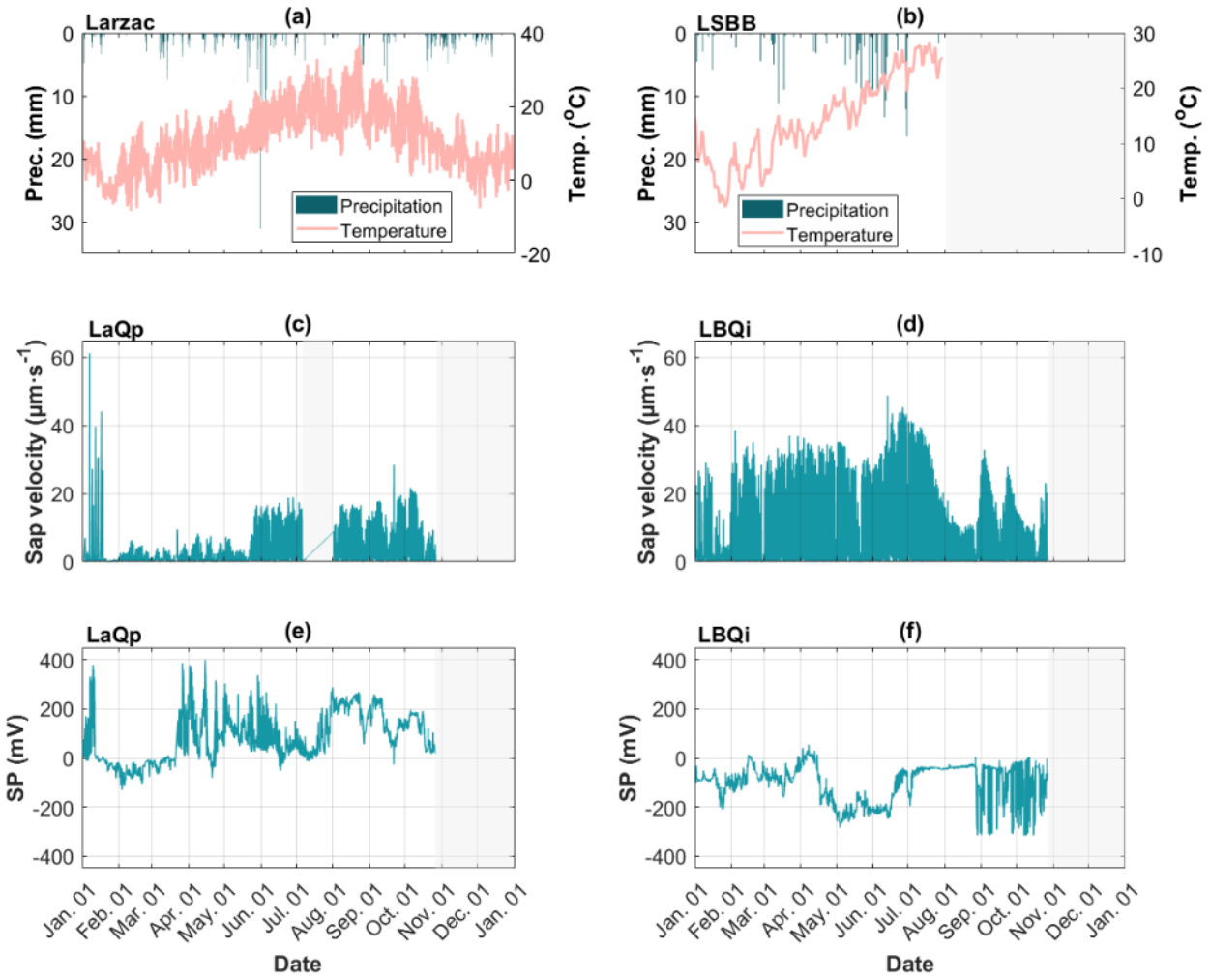

Figure S3: One-year data collected at the Larzac and LSBB sites from January 1, 2023, to January 1, 2024. (a–b) Precipitation and air temperature data; (c–d) Sap velocity for the Pubescent oak (LaQp) and the Holm oak (LSQi), respectively; (e–f) SP measurements for LaQp and LSQi, respectively. The grey shaded areas indicate periods with missing data.

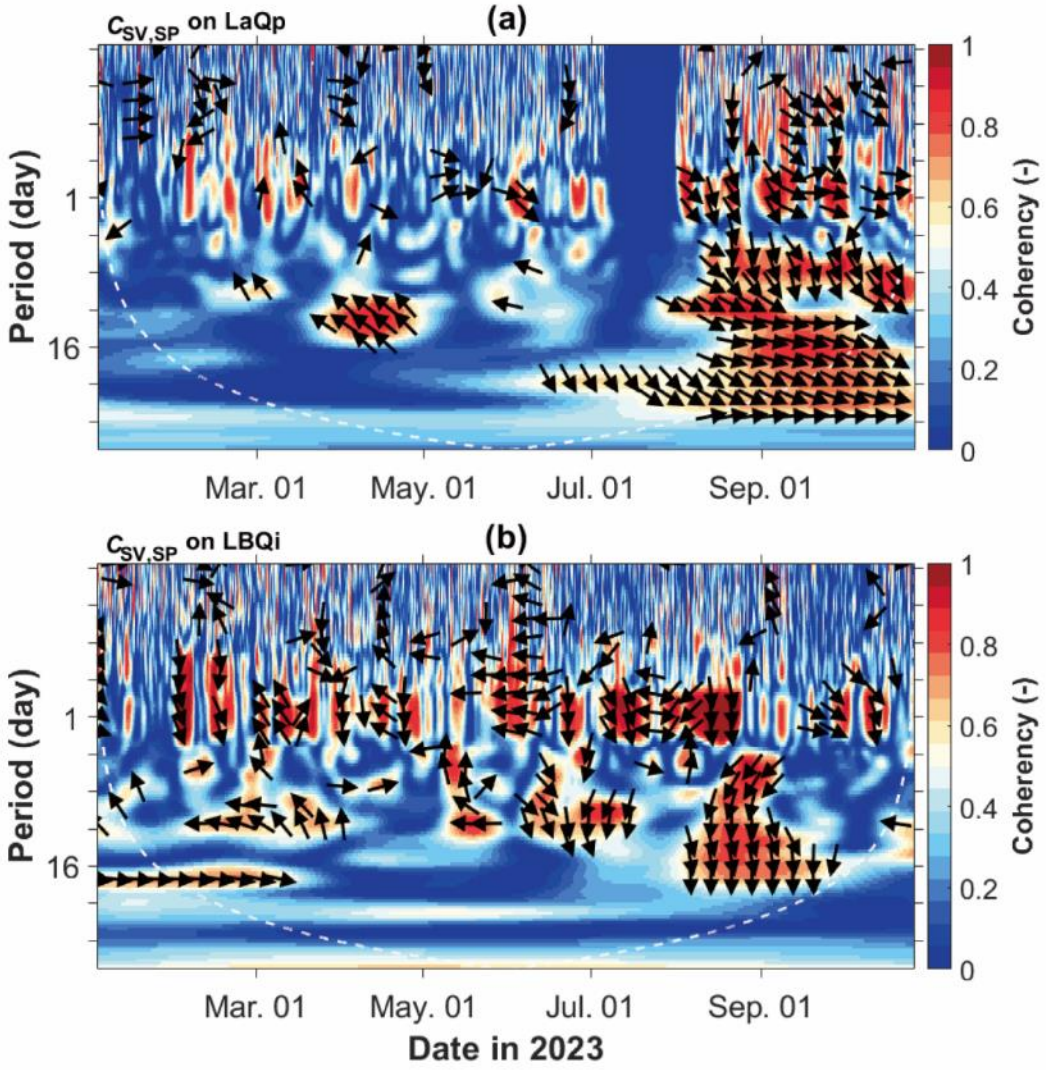

Figure S4: Wavelet coherence analysis between sap velocity and SP data on the Pubescent oak (LaQp) at the Larzac site (a), and the Holm oak (LSQi) at the LSBB site (b), respectively; Arrows denote the lag/lead phase between the two time series; White dashed lines indicate the cone of influence where edge artifacts are negligible.

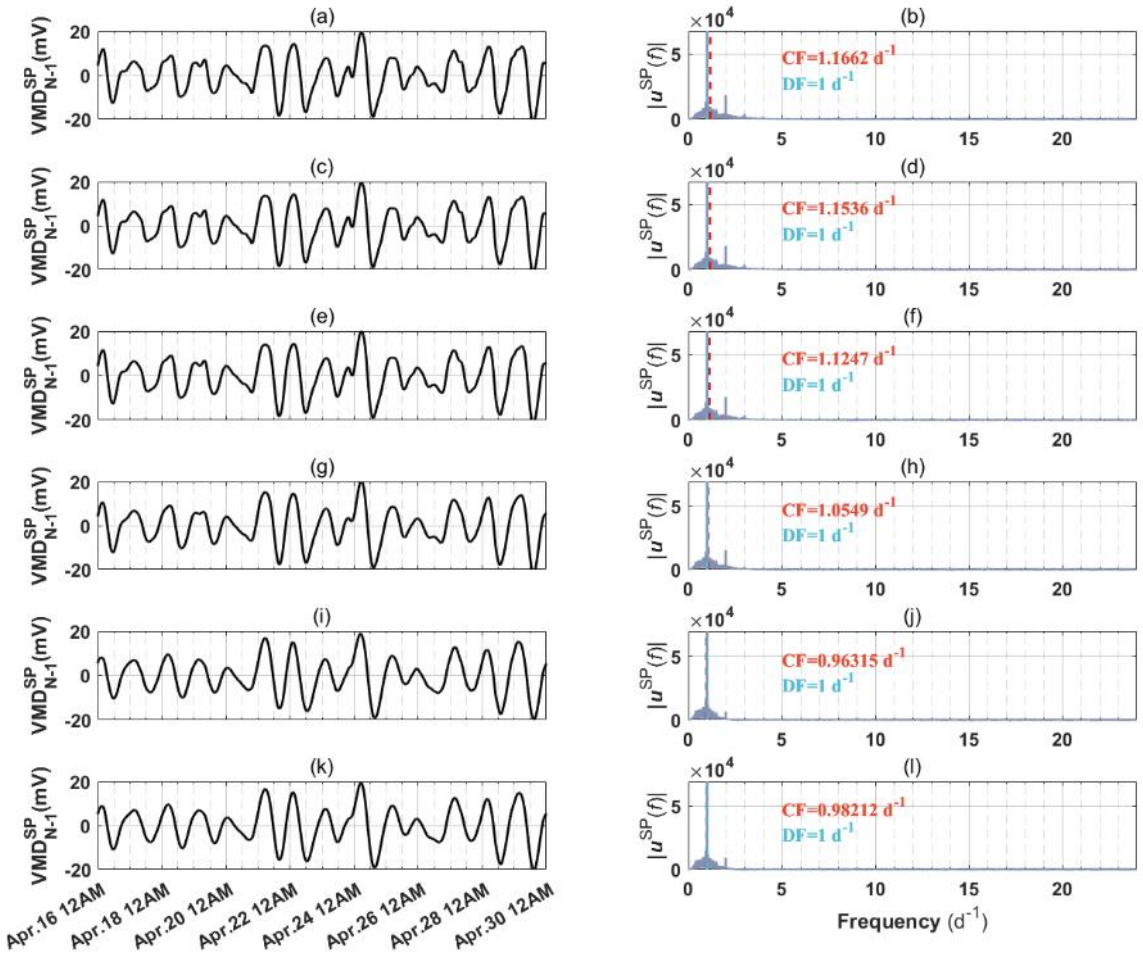

Figure S5: (left column: a, c, e, g, i, k) The second-last decomposed modes of tree SP data obtained for the Holm oak at the Font-Blanche site (FBQi) and (right column: b, d, f, h, j, l) their corresponding frequency spectra. The total number of modes *N* used to decompose the data are 7, 8, 9, 10, 11, and 12 from the (a–b) top to the (k–l) bottom.

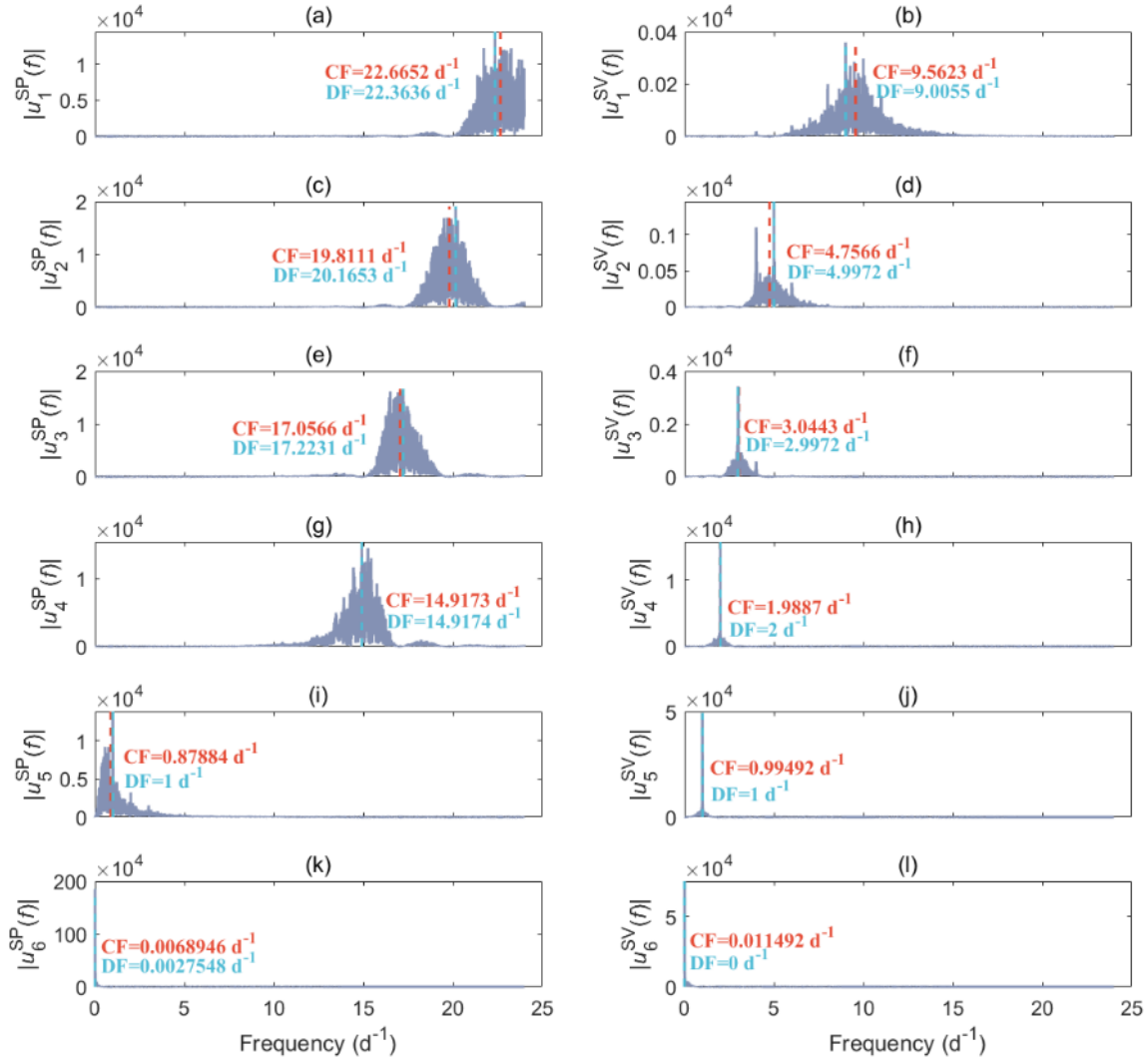

Figure S6: Frequency spectra of six decomposed modes of (left column: a, c, e, g, i, k) tree SP and (right column: b, d, f, h, j, l) sap velocity data obtained on the Aleppo pine at the Font-Blanche site (FBPh) within 2023 using VMD; Different rows correspond to different modes, where "CF" and "DF" indicate the central frequency and dominant frequency of the corresponding mode, respectively.

Figure S7: The correlation coefficients of the VMD-filtered data at diurnal time scales at the Font-Blanche site in April 16–30, 2023

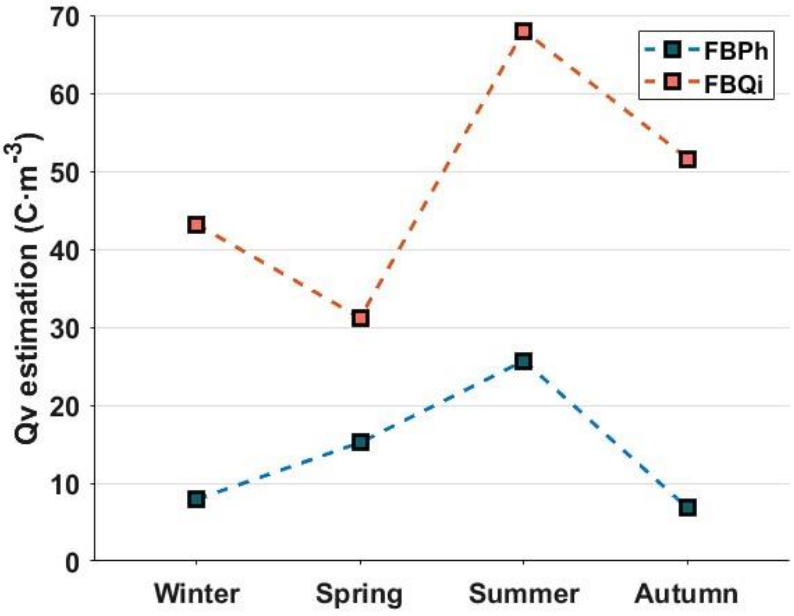

Figure S8: Estimated $\widehat{Q}_v$ values during periods (two weeks) without rainfall across four seasons in 2023 for FBPh and FBQi (refer to Table S2).

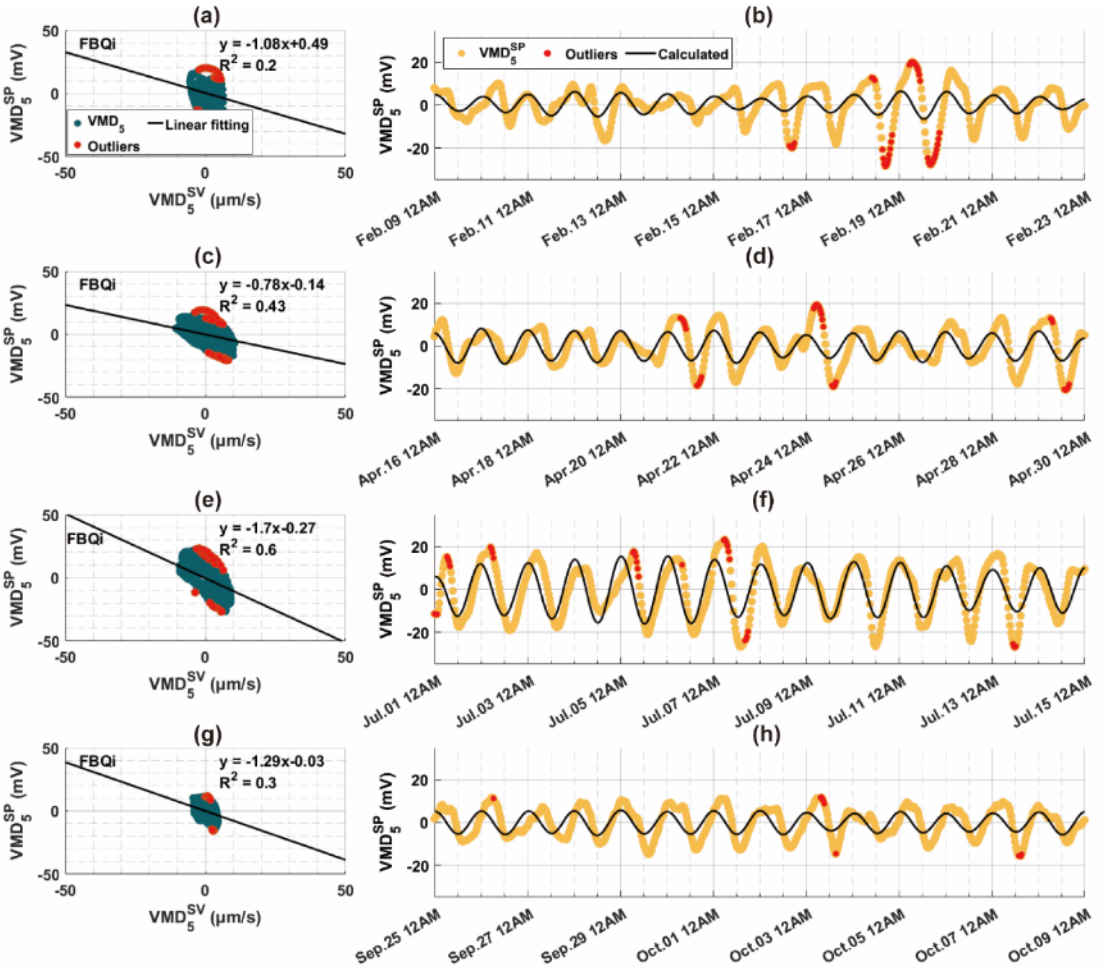

Figure S9: The relationship between the fifth decomposed modes of sap velocity (VMD_5^{SV}) and tree SP (VMD_5^{SP}) signals in (a–b) winter, (c–d) spring, (e–f) summer, and (g–h) autumn of 2023 for the Holm oak (FBQi) at the Font-Blanche site. (a, c, e, f) Scatter plots of the decomposed modes of sap velocity and SP signals with black lines indicating linear regression results and red dots indicating points (outliers) outside the 95% confidence level of the regression. (b, d, f, h) Corresponding decompositions of SP signals (orange dots) and calculated SP (black lines) based on the linear relationship between VMD_5^{SV} and VMD_5^{SP}, with red dots as outliers outside the 95% confidence level of the linear regression.

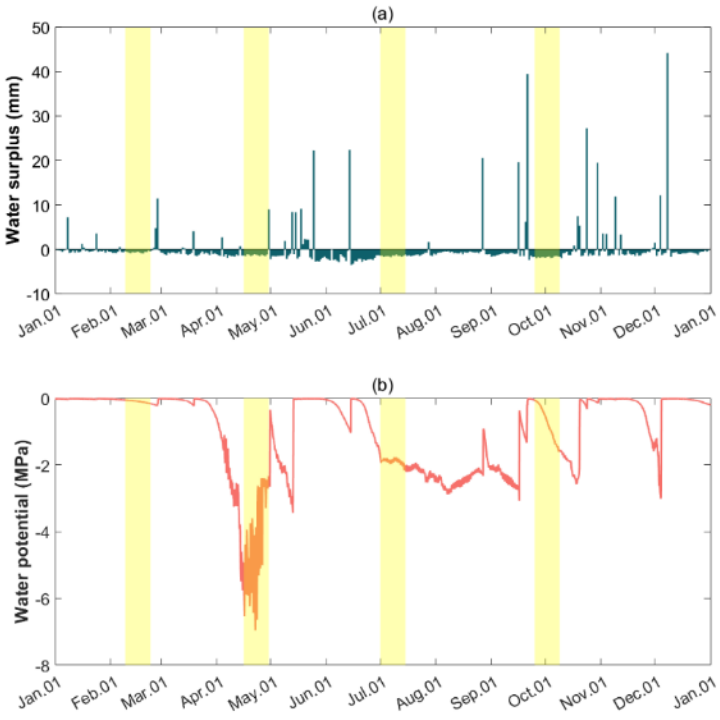

Figure S10: The water surplus and soil matric potential in vicinity of tree from Jan. 01, 2023, to Jan. 01, 2024, at the Font-Blanche site. Yellow shaded areas represent the selected periods within different seasons.

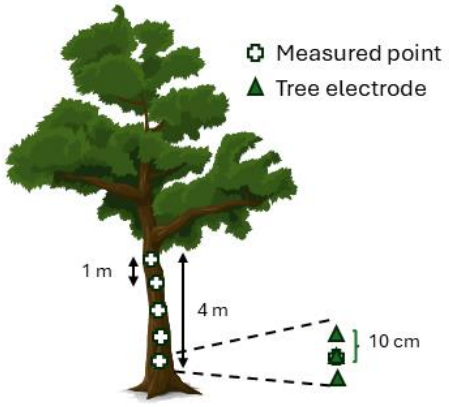

Figure S11: Schematic diagram of tree electrode configuration.

Table S1 Parameters of measurements and the corresponding sampling time interval and units.

Site / Parameter	Larzac		LSBB		Font-Blanche	
	Time interval	Unit	Time interval	Unit	Time interval	Unit
Tree SP	1 min	mV	1 min	mV	10 min	mV
Sap velocity	30 min	$\mu m \cdot s^{-1}$	30 min	$\mu m \cdot s^{-1}$	30 min	$\mu m \cdot s^{-1}$
Precipitation	1 h	mm	24 h	mm	30 min	mm
Air temperature	1 h	ºC	24 h	ºC	30 min	ºC
VPD	/	/	/	/	30 min	Pa
Actual ET	/	/	/	/	30 min	mm

Table S2 Seasonal characteristics of two-week (Feb. 09–23, Apr. 16–30, Jul. 01–15, and Sep. 25–Oct. 09) data for the Aleppo pine (FBPh) and Holm oak (FBQi) at the Font-Blanche site.

Season	**Property**		**FBPh**	**FBQi**
Winter	Range	VMD_5^{SP} (mV)	[−4.78, +3.90]	[−21.81, +17.83]
		VMD_5^{SV} (μm·s^{-1})	[−10.56, +9.86]	[−5.61, +6.49]
	Standard Deviation	VMD_5^{SP} (mV)	1.89	7.13
		VMD_5^{SV} (μm·s^{-1})	5.49	3.00
	$\hat{Q}_v$ (C·m^{-3})		7.9	43.2
	Correlation Coefficient		0.83	0.45
Spring	Range	VMD_5^{SP} (mV)	[−5.57, +4.69]	[−19.52, +16.04]
		VMD_5^{SV} (μm·s^{-1})	[−6.29, +6.36]	[−10.60, +10.61]
	Standard Deviation	VMD_5^{SP} (mV)	2.28	7.51
		VMD_5^{SV} (μm·s^{-1})	3.61	6.33
	$\hat{Q}_v$ (C·m^{-3})		15.2	31.2
	Correlation Coefficient		0.88	0.66
Summer	Range	VMD_5^{SP} (mV)	[−5.58, +5.93]	[−26.82, +22.35]
		VMD_5^{SV} (μm·s^{-1})	[−4.22, +4.09]	[−9.36, +9.32]
	Standard Deviation	VMD_5^{SP} (mV)	2.24	11.94
		VMD_5^{SV} (μm·s^{-1})	2.15	5.43
	$\hat{Q}_v$ (C·m^{-3})		25.7	68.0
	Correlation Coefficient		0.91	0.77
Autumn	Range	VMD_5^{SP} (mV)	[−5.94, +5.06]	[−14.73, +11.81]
		VMD_5^{SV} (μm·s^{-1})	[−10.90, +10.89]	[−4.48, +4.68]
	Standard Deviation	VMD_5^{SP} (mV)	2.44	6.68
		VMD_5^{SV} (μm·s^{-1})	6.68	2.82
	$\hat{Q}_v$ (C·m^{-3})		6.8	51.6
	Correlation Coefficient		0.69	0.54